Journal of Medicinal Chemistry

Article

Total Synthesis of Two Novel Subpicomolar Sarco/Endoplasmatic Reticulum Ca-ATPase Inhibitors Designed by an Analysis of the Binding Site of Thapsigargin

Helmer Shoel, Tommy Liljefors, Steven V. Ley, Steven F. Oliver, Alessandra Antonello, Martin D Smith, Carl Erik Olsen, John T. Isaacs, and S. Brgger Christensen

J. Med. Chem., **2005**, 48 (22), 7005-7011• DOI: 10.1021/jm058036v • Publication Date (Web): 04 October 2005

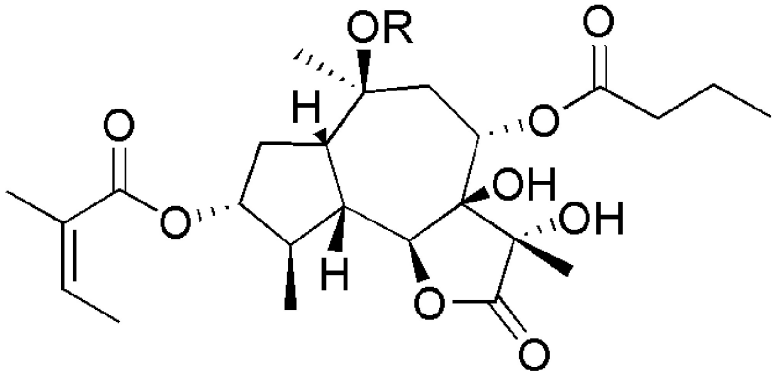

$R = C_2H_5$; $R = OCCH_3$

More About This Article

Additional resources and features associated with this article are available within the HTML version:

- Supporting Information
- Links to the 3 articles that cite this article, as of the time of this article download
- Access to high resolution figures
- Links to articles and content related to this article
- Copyright permission to reproduce figures and/or text from this article

View the Full Text HTML

Journal of Medicinal Chemistry is published by the American Chemical Society. 1155 Sixteenth Street N.W., Washington, DC 20036

Total Synthesis of Two Novel Subpicomolar Sarco/Endoplasmatic Reticulum Ca^{2+}-ATPase Inhibitors Designed by an Analysis of the Binding Site of Thapsigargin

Helmer Søhoel,[†] Tommy Liljefors,[†] Steven V. Ley,*[,‡] Steven F. Oliver,[‡] Alessandra Antonello,[‡] Martin D Smith,[‡] Carl Erik Olsen,[§] John T. Isaacs,[⊥] and S. Brøgger Christensen*[,†]

Department of Medicinal Chemistry, The Danish University of Pharmaceutical Sciences, Universitetsparken 2, DK-2100 Copenhagen Ø, Denmark, Department of Chemistry, University of Cambridge, Lensfield Road, Cambridge CB2 1EW, United Kingdom, Department of Natural Sciences, The Royal Veterinary and Agricultural University, Bülowsvej 17, DK-1870 Frederiksberg C, Denmark, and The Sidney Kimmel Comprehensive Cancer Center at Johns Hopkins, Baltimore, Maryland 21231

Received June 21, 2005

Analysis of molecular interaction fields based on the published crystal structure of thapsigargin bound to the sarco/endoplasmatic reticulum Ca^{2+}-ATPase and analysis of the volume and shape of the ligand binding site and of the SERCA−thapsigargin interactions have enabled design of two new compounds inhibiting SERCA in the subpicomolar range. The two inhibitors were synthesized using (*S*)-carvone as starting material and found to be 3 and 10 times more potent than thapsigargin.

Introduction

The remarkably low proliferation rate of androgen-independent prostate cancer cells makes conventional chemotherapy ineffective and consequently no current treatment prolongs survival in men suffering from this disease.[1,2] The sesquiterpene lactone Thapsigargin (Tg, **1**) (Chart 1), first isolated in 1978 from the medicinal plant *Thapsia garganica* L.,[3] provokes programmed cell death in both proliferative and quiescent cells[4] including androgen-independent prostate cancer cells.[5]

The mechanism of action behind the apoptosis provoked by Tg is an inhibition of the sarco/endoplasmatic reticulum Ca^{2+}-ATPase (SERCA) causing a rise of the cytosolic Ca^{2+} level eventually leading to cell death.[6] The SERCA pumps remove Ca^{2+} against a concentration gradient from the cytosol to the endo/sarcoplasmatic reticulum. During the transport of Ca^{2+} the SERCA pumps adopts a number of very different conformations,[7−11] but only one of these, the E2 conformation, shows affinity for Tg. Tg inhibits SERCA with a dissociation constant of ≤2.2 pM,[12,13] but at present Tg can only be obtained from the fruits and roots of the noncultivated Mediterranean plant *Thapsia garganica*.[14] However, designed Tg analogues that may be SERCA inhibitors can be obtained through total synthesis, exploiting the recently published 3D-structure of the SERCA−Tg complex.[8]

The present work demonstrates that analysis of the binding site using molecular interaction fields calculated by the program GRID,[15] analysis of the volume and shape of the ligand binding site using the program PASS,[16] and analysis of the interactions between the ligand and the protein enabled the design of two new small molecule inhibitors of SERCA. The two new molecules were synthesized and evaluated as SERCA inhibitors.

Chart 1

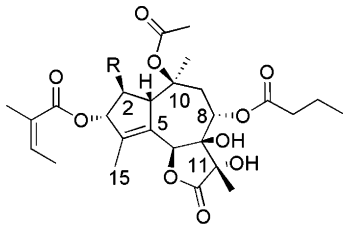

1 R = $OOC(CH_2)_6CH_3$
2 R = H

Results and Discussion

GRID Contour Maps for Favorable Hydrophilic Interactions. Favorable hydrophilic regions of SERCA within the binding site of Tg were explored using the water probe (OH2). GRID calculations were performed both with and without Tg for an extensive investigation the hydrophilic character of the binding site (Figure 1).

The GRID analysis of the binding site after removal of Tg (Figure 1a) reveals energetically favorable binding sites for water molecules (contours W1, W2, and W3) which are not present when Tg is included in the calculations (Figure 1b) indicating that a number of water molecules are displaced as Tg binds.

Since none of the hydrogen bond donating and accepting sites of Tg coincide with any of the contours in Figure 1a, this indicates that Tg does not have any strong direct hydrogen bond interactions with SERCA. The only direct interaction is a weak hydrogen bond from the backbone NH of Ile829 to the carbonyl group of the butanoyl group at O-8 with a heavy-atom distance between the hydrogen donor and acceptor of 3.48 Å

* Correspondence regarding synthetic chemistry should be addressed to S.V.L.: Tel.: +44 1223 336402. Fax: +44 1223 336442. E-mail: svl1000@cam.ac.uk. All other correspondence should be addressed to S.B.C.: Tel.: +45 3530 6253. Fax: +45 3530 6041. E-mail: sbc@dfuni.dk.
[†] The Danish University of Pharmaceutical Sciences.
[‡] The University of Cambridge.
[§] The Royal Veterinary and Agricultural University.
[⊥] Johns Hopkins.

10.1021/jm058036v CCC: $30.25
Published on Web 10/04/2005

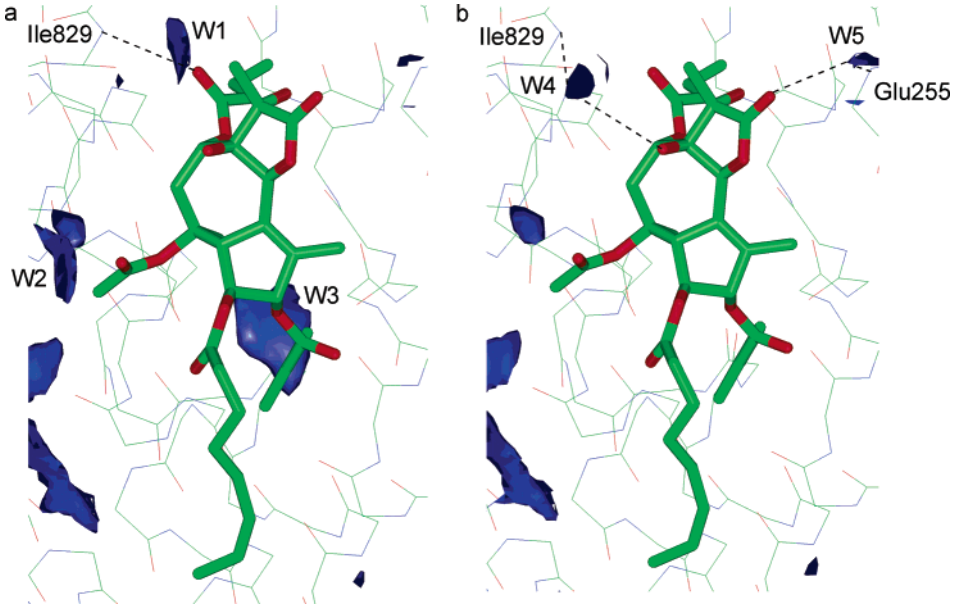

Figure 1. Molecular interaction fields calculated for a water probe and contoured at −7 kcal/mol. (a) Calculations without ligand, (b) calculations including the ligand.

(Figure 1a). The GRID study of the binding site with Tg bound (Figure 1b) reveals a new water contour W4 (Figure 1b). It should, in this context, be noted that the experimentally determined structure of the SERCA−Tg complex does not contain any resolved water molecules.[8] The calculated contours in Figure 1b indicate probable positions of water molecules in the ligand−protein complex. The 7-OH group and the C-12 carbonyl group of Tg may interact indirectly with SERCA via water molecules located in regions W4 and W5. It is surprising that such a highly oxygenated molecule as Tg only interacts with the protein via one direct (but weak) hydrogen bond and possibly by two water-mediated hydrogen bonds.

GRID Contour Map for Favorable Lipophilic Interactions. Regions of favorable lipophilic interactions within the binding site of Tg were explored using the methyl probe (C3) in the absence of Tg (Figure 2).

The five regions L1, L2, L3, L4, and L5 in Figure 2 are regions of energetically favorable lipophilic interactions. Other analyses also indicate that the affinity of Tg for SERCA mainly is determined by lipophilic interactions.[17,18] It is notable that the tricyclic framework of Tg apparently only serves as a scaffold positioning the five lipophilic moieties (O-8 butanoyl, C-15, O-3 angeloyl, O-2 octanoyl, and O-10 acetyl) in such a way that they can interact with the lipophilic regions L1, L2, L3, L4, and L5, respectively (Figure 2). The major part of the strong affinity of Tg to the binding site of SERCA is most probably due to these intermolecular lipophilic interactions. It should, however, be noted that the O-2 octanoyl group only coincides with the very small lipophilic region L4 in Figure 2, indicating a minor role of this group for the affinity of Tg. This is supported by the high affinity of nortrilobolide (**2**) which lacks the octanoyl group (unpublished).

In conclusion, this GRID analysis of the Tg binding to SERCA reveals an overall lipophilic character involving the lipophilic regions L1, L2, L3, and L5.

Putative Active Sites Spheres (PASS) Visualization of the Tg Cavity.[19] A comparison of the shape of the cavity, in which Tg is bound, with the van der Waals surface of Tg reveals a high degree of complementarity (Figure 3). The very close fit between the cavity and the ligand and indicates that the shape and volume of the cavity is to a large degree induced by Tg when it binds to SERCA. Consequently, in the design of novel compounds binding to the Tg binding site, the scaffold should be as rigid as possible and similar to Tg with respect to shape and volume.

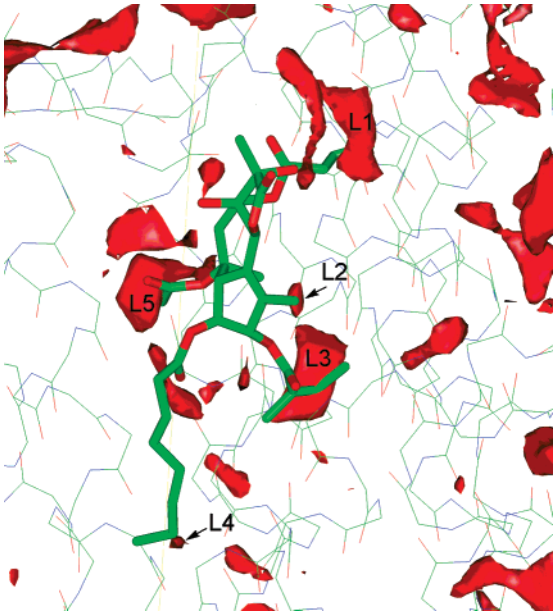

Figure 2. Molecular interaction fields calculated for a methyl probe and contoured at −3 kcal/mol.

Design of New Inhibitors. The synthesis of compound **3** has been previously described from (*S*)-carvone;[20] **3** should easily be converted into **4** and **5** (Scheme 1). The tricyclic structure of the two analogues limits their flexibility, and docking the lowest energy minima of **4** and **5** disclose coincidence of O-8 butanoyl, C-15, O-3 angeloyl, and O-10 acetyl with the lipophilic L1, L2, L3, and L5 regions, respectively (Figure 4).

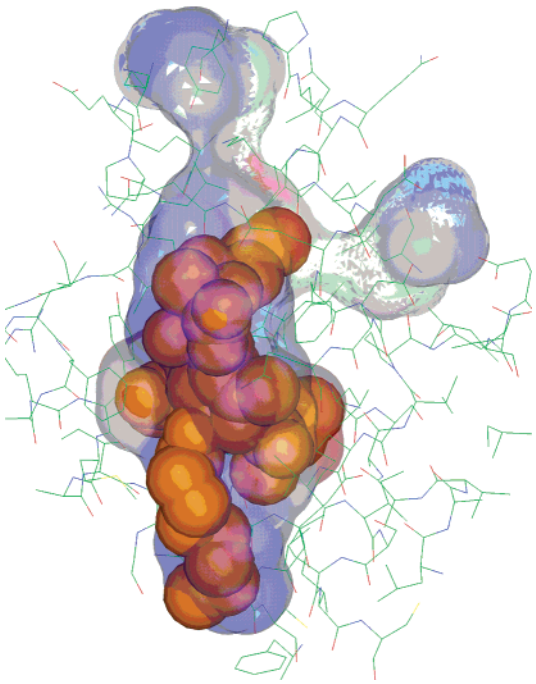

Figure 3. Pass visualization of the volume and shape of the binding site of Tg. The orange sphere depicts the van der Waals volume of Tg.

Scheme 1[a]

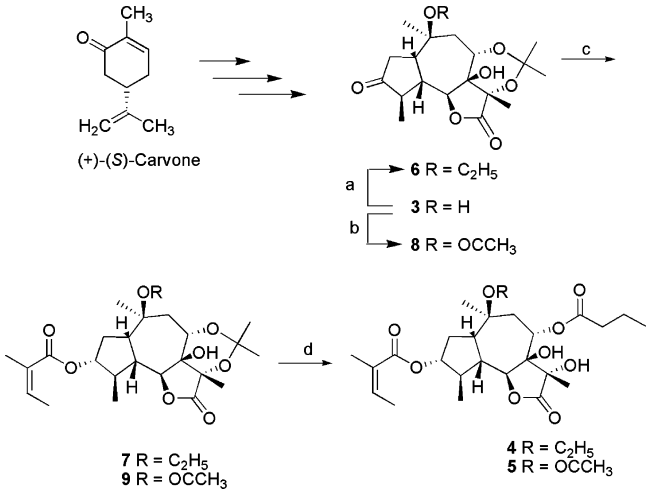

[a] Reagents and conditions: (a) $(CH_3)_3COK$, CH_3CH_2Br, DMF, room temperature, 2 h, yield 71%. (b) $(CH_3CO)_2O$, DCM, DIPEA, DMAP, room temperature, 6 h, yield 89%.[20] (c) (1) $NaBH_4$, MeOH (dry), 0 °C, 30 min. (2) Angelic acid, 2,4,6-trichlorobenzoyl chloride, Et_3N, toluene, room temperature, 20 h, yield over two steps **7**: 71%, **9**: 98%. (d) (1) HCl, MeOH, 45 °C, 4 h. (2) Butyric anhydride, DCM, DMAP, room temperature, 30 min., yield over two steps **4**: 82%, **5**: 63%.

Furthermore an analysis of the shape and volume of **4** and **5** reveals that these molecules will fit into the cavity formed by Tg.

An Unfavorable Electrostatic Interaction between Tg and SERCA. Inspection of the binding of Tg to SERCA reveals an unfavorable electrostatic interaction between the phenyl ring of Phe834 of SERCA and the carbonyl group of the acetyl group at O-10 of Tg. The carbonyl oxygen is positioned 2.8 Å right below the phenyl ring of Phe834 (Figure 5), causing a repulsive electrostatic interaction between the negative electrostatic potential below (and above) the face of the

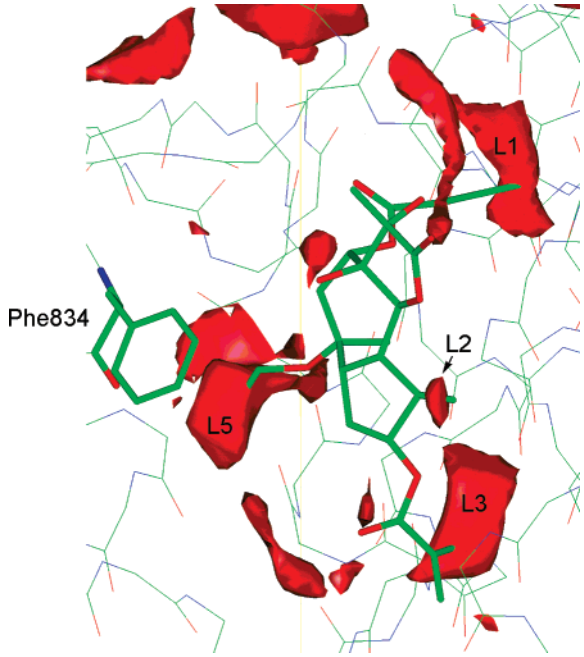

Figure 4. The global minimum conformation of **4** docked into the binding site of Tg. Red contours depict calculated favorable lipophilic regions contoured at −3 kcal/mol.

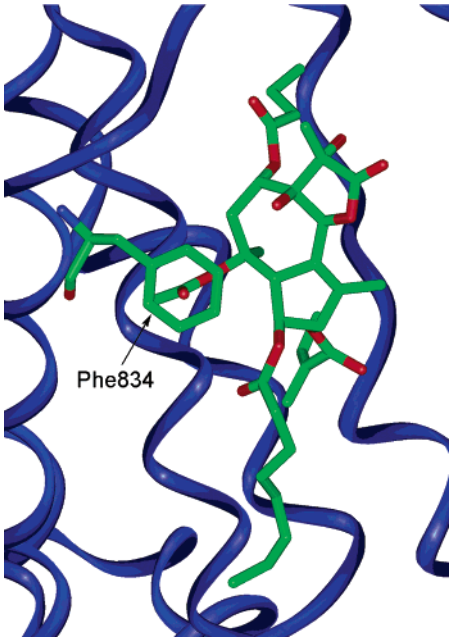

Figure 5. Unfavorable interaction between Tg and Phe834 of SERCA.

phenyl ring and the carbonyl oxygen carrying a partial negative charge.

The origin of this interaction in Tg is due to the presence of the double bond between C-4 and C-5 and of three antiparallel carbonyl dipoles (at O-2, O-3, and O-10); this prevents the acetyl carbonyl adopting an orientation in which the electrostatic repulsion between the carbonyl at O-10 and the phenyl ring of Phe834 is relieved.

The absence of the carbonyl group in the side chain attached to C-10 in **4** removes the unfavorable electrostatic interaction with the Phe834 (Figure 4), and a higher affinity than that of Tg is consequently expected. More interesting, however, is that a comparison between

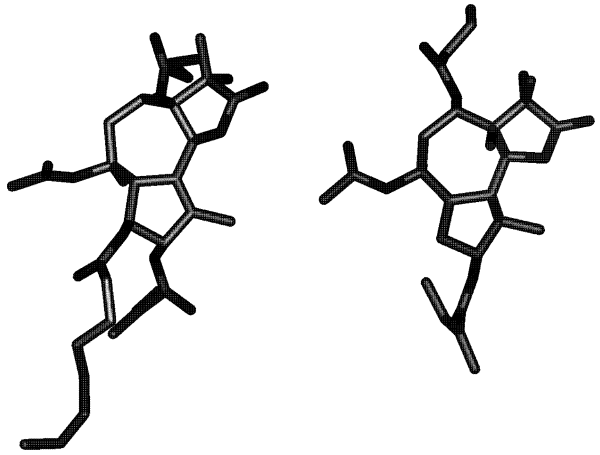

Figure 6. Illustration of Tg (left) as bound to SERCA and the calculated lowest energy minimum of **5** (right).

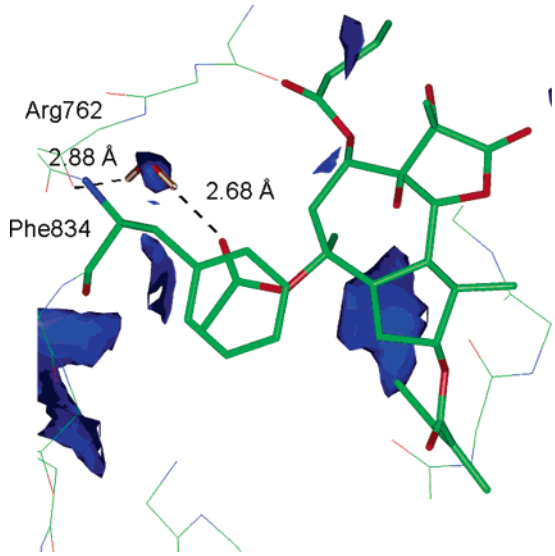

Figure 7. The global energy minimum conformation of **5** docked into the binding site of Tg. Blue contours depict favorable hydrophilic regions −7 kcal/mol. A water molecule placed in a hydrophilic GRID area can interact with the carbonyl of the acetyl group and the backbone carbonyl of Arg762.

the calculated lowest energy minima of **5** and Tg discloses different orientations of the C-10 ester group in the two compounds (Figure 6).

The orientation of the carbonyl group in the conformation adopted by **5** should not cause electrostatic repulsion with Phe834 in the binding site of SERCA. A corresponding carbonyl group orientation is not accessible to Tg as the conformational analysis indicates that this conformation of Tg is 5 kcal/mol higher in energy than the conformation observed in the X-ray crystal structure.

The docking of **5** into SERCA (Figure 7) reveals that the orientation of the C-10 ester not only eliminates the electrostatic repulsion with Phe834 but also generates an electrostatic attraction (cation−π interaction), due to the partial positive charge on the carbonyl carbon and its location right below the phenyl ring. Furthermore, the C-10 ester group conformation in **5** enables the carbonyl oxygen of Arg762 to form a hydrogen bond mediated by water (dashed line in Figure 7). Encouraged by these conclusions we decided to synthesize compound **4** and **5**.

Table 1. SERCA Activities of **4** and **5** Relative to Tg

compound	SERCA inhibition[a]
Tg	1.0
4	0.3
5	0.1

[a] Relative potencies are stated (IC_{50} Analogue/IC_{50} Tg) for inhibition of SERCA. The figures are mean of two experiments each performed in triplicate.

Chemistry. The total synthesis of the Tg analogues **4** and **5** (Scheme 1) took advantage of the method, previously described for conversion of (+)-(*S*)-carvone into **3** in 29 steps.[20,21]

The expected poor reactivity of the 7-OH group in **3** due to steric hindrance made protection unnecessary (Scheme 1). Accordingly, *tert*-butoxide-promoted alkylation with ethyl bromide afforded selective O-10 ethylation to give **6** in a yield of 71%. Reduction of the ketone at C-3 with sodium borohydride selectively provided the *R*-secondary alcohol, and Yamaguchi esterification[22] of the 3-OH with angelic acid gave **7** in an overall yield of 71% (from **3**). Acid-catalyzed removal of the acetonide and selective esterification of O-8 with butyric anhydride in the presence of 4-(dimethylamino)pyridine (DMAP) afforded the target compound **4** in a total yield of 82% in the last two steps. The Tg analogue **5** was made from the 8-*O*-debutanoyl synthon analogous to a previously described procedure[12] but esterifying O-8 with the use of butyric anhydride instead of 2-methylbutyric anhydride.

Measurement of ATPase Activity. The SERCA activity was measured indirectly by a coupled enzyme assay as the rate of ATP hydrolysis.[23,24] Decreased SERCA activity was used as a measurement of the inhibitory potency of the agents. The SERCA inhibitory activities of Tg and the analogues **4** and **5** are given in Table 1.

Ligands **4** and **5** were three and 10 times more potent than Tg, respectively.

Conclusion

A computational analysis of the binding site of Tg in the SERCA−Tg complex has revealed interactions of importance for the affinity between Tg and SERCA. On the basis of this analysis, two new SERCA inhibitors were designed and synthesized. The biological response study disclosed that the inhibitors were 3 and 10 times more potent than Tg. Consequently we have shown that design and synthesis of simplified SERCA inhibitors is viable from readily available (+)-(*S*)-carvone.

Experimental Section

Chemistry. All reactions were performed under an argon atmosphere. Glassware was dried by heating in an oven at a temperature above 125 °C for at least 6 h. Rotary evaporation was performed under reduced pressure (min. 25 mbar) and at maximum temperature 40 °C. High vacuum refers to a pressure of approximate 2 mmHg.

Petrol refers to the fraction of light petroleum ether bp (40−60 °C). Dichloromethane (DCM) was distilled from calcium hydride, and methanol was distilled from magnesium methoxide. All other reagents and solvents were purified by standard procedures or used as obtained from the supplier. All reactions were followed by thin-layer chromatography

(TLC). Analytical TLC was performed on precoated aluminum sheets Merck Silica Gel 60 F_{254}. Column chromatography was carried out using Merck Kieselgel 60 (230−400 mesh). Compounds were visualized by quenching of UV fluorescence (λ = 254 nm), by staining with a 1% naphthoresorcinol solution in ethanolic sulfuric acid (1 M) or by an acidic ammonium molybdate(IV) solution and visualized by heating. Optical rotations were measured using a Perkin-Elmer 241 Polarimeter. ^{1}H NMR and ^{13}C NMR spectra were recorded on a Bruker DRX 500 or a Varian Mercury 300 instrument at room temperature. Abbreviations used for multiplicities: br = broad signal, s = singlet, d = doublet, t = triplet, and q = quartet, p = pentet. The signal of the solvent was used as an internal reference. Asterisk-marked shifts may be interchanged. COSY, NOESY, HMBC, and HMQC spectra were used for assignment of the NMR signals.

(2a*S*,5a*S*,7*S*,7a*S*,10*R*,10a*S*,10b*S*,10c*R*)-7-Ethoxy-10c-hydroxy-2a,4,4,7,10-pentamethyl-octahydro-1,3,5-trioxabenzo[*cd*]cyclopenta[*h*]azulene-2,9-dione (6). Potassium *tert*-butoxide (2.4 mg, 0.2 mmol) and after 20 min ethyl bromide (153.9 mg, 1.4 mmol) were added at room temperature to a stirred solution of diol **3** (25 mg, 0.07 mmol) in dry *N,N*-dimethylformamide (1 mL). After being stirred for additional 2 h, the reaction was quenched with a half saturated solution of $NaHCO_3$ (1 mL). The aqueous layer was extracted with DCM (3 × 5 mL). The combined organic layers were dried ($MgSO_4$), and the solvent was removed under reduced pressure. The crude product was purified by flash chromatography (petrol/EtOAc, 2:1) to yield ethyl ether **6** (19 mg, 71%) as colorless oil. $[\alpha]^{25}_D$ +17.9 (*c* 0.23, $CHCl_3$). ^{1}H NMR (300 MHz, $CDCl_3$) δ 4.49 (1H, d, J = 10.8 Hz, H-6), 4.07 (1H, dd, J = 5.7, 7.5 Hz, H-8), 3.61 (1H, p, J = 7.2 Hz, ethyl ether H-1), 3.51 (1H, p, J = 7.2 Hz, ethyl ether H-1′), 2.81−2.70 (2H, m, H-1, H-4), 2.51 (2H, m, H-5, H-9), 2.28−2.21 (1H, m, H-2), 2.20−2.16 (1H, m, H-2′), 1.63 (1H, dd, J = 5.7, 17.1 Hz, H-9′), 1.47 (3H, s, acetonide CH_3), 1.45 (3H, s, acetonide CH_3), 1.31 (3H, s, H-13), 1.23 (3H, s, H-14), 1.14−1.19 (6H, d, m, H-15, ethyl ether H-2). ^{13}C NMR (75 MHz, $CDCl_3$) δ 218.9 (C-3), 174.3 (C-12), 99,2 (acetal C), 79.6* (C-7), 79.5* (C-6), 79.2* (C-10), 77.6* (C-11), 67.0 (C-8), 58.3 (ethyl ether C-1), 47.8 (C-1), 44.3 (C-5), 43.2 (C-4), 40.2 (C-9), 38.6 (C-2), 30.9 (acetonide CH_3), 27.5 (ethyl ether C-2), 24.1 (acetonide CH_3), 18.9 (C-14), 17.2 (C-13), 15.6 (C-15).

(*Z*)-2-Methyl-but-2-enoic Acid (2a*S*,5a*S*,7*S*,7a*S*,9*R*,10*R*,-10a*R*,10b*S*,10c*R*)-7-Ethoxy-10c-hydroxy-2a,4,4,7,10-pentamethyl-2-oxo-dodecahydro-1,3,5-trioxa-benzo[*cd*]cyclopenta[*h*]azulen-9-yl Ester (7). $NaBH_4$ (11.5 mg, 0.3 mmol) was added at 0 °C to a stirred solution of ketone **6** (12 mg, 0.03 mmol) in dry methanol (0.5 mL). After stirring at 0 °C for 30 min, no starting material could be detected and a half-saturated solution of $NaHCO_3$ (1 mL) was added. The aqueous layer was extracted with DCM (3 × 5 mL). The combined organic layers were dried ($MgSO_4$), and the solvent was removed under reduced pressure providing the crude diol (13 mg) as white foam. The product was used directly in the next step. 2,4,6-Trichlorobenzoyl chloride (268.4 mg, 1.1 mmol) and triethylamine (110.0 mg, 1.1 mmol) were added at room temperature to a stirred solution of angelic acid (108.8 mg, 1.1 mmol) in toluene (0.5 mL). The solution was stirred at room temperature for 2 h. A premixed solution of the crude diol (13 mg) in toluene (0.5 mL) was added, and the mixture was stirred at 75 °C for additional 18 h. After being cooled to room temperature, the reaction mixture was quenched with a half-saturated solution of $NaHCO_3$ (2 mL). The aqueous layer was extracted with diethyl ether (3 × 5 mL). The combined organic layers were dried ($MgSO_4$), and the solvent was removed under reduced pressure. The residue was purified by flash chromatography (petrol/EtOAc, 2:1) to yield 7 (71% over two steps) as a colorless oil; $[\alpha]^{25}_D$ −41.9 (*c* 0.14, $CHCl_3$). ^{1}H NMR (300 MHz, $CDCl_3$) δ 6.02 (1H, qq, J = 1.5, 7.2 Hz, angeloyl H-3), 4.87−4.77 (1H, m, H-3), 4.97 (1H, d, J = 11.7 Hz, H-6), 4.03 (1H, t, J = 6.9 Hz, H-8), 3.56 (1H, p, J = 6.9 Hz, ethyl ether H-1), 3.45 (1H, p, J = 6.9 Hz, ethyl ether H-1′), 2.62−2.52 (1H, m, H-4), 1.44−1.32 (2H, m, H-1, H-9), 2.11−2.08 (1H, m, H-5), 1.93 (3H, dq, J = 1.5, 7.2 Hz, angeloyl H-4), 1.81 (3H, p, J = 1.5 Hz, angeloyl C-2 CH_3), 1.63(1H, dd, J = 6.8, 16.2 Hz, H-9′), 1.47 (3H, s, acetonide CH_3), 1.44 (3H, s, acetonide CH_3), 1.39−1.32 (1H, m, H-2), 1.35−1.31 (1H, m, H-2′), 1.28 (3H, s, H-13), 1.22−1.14 (9H, m, H-14, H-15, ethyl ether H-2). ^{13}C NMR (75 MHz, $CDCl_3$) δ 174.8 (C-12), 168.0 (angeloyl, C═O), 138.9 (angeloyl, C-3), 128,0 (angeloyl, C-2), 98.9 (acetal C), 80.5* (C-7), 79.9* (C-6), 79.6* (C-3), 79.5* (C-11), 77.7* (C-10), 67.4 (C-8), 58.0 (ethyl ether, C-1), 46.6 (C-1), 44.6 (C-5), 43.3 (C-4), 37.7 (C-9), 35.8 (C-2), 30.9 (acetonide, CH_3), 27.4 (ethyl ether, C-2), 24.1 (acetonide, CH_3), 21.1 (angeloyl, C-2 *C*H_3), 19.7 (C-14), 18.2 (C-13), 16.3 (angeloyl, C-4), 15.7 (C-15).

(Z)-2-Methyl-but-2-enoic Acid (3*S*,3a*R*,4*S*,6*S*,6a*S*,8*R*,9*R*,-9a*R*,9b*S*)-4-Butyryloxy-6-ethoxy-3,3a-dihydroxy-3,6,9-trimethyl-2-oxo-dodecahydro-azuleno[4,5-*b*]furan-8-yl Ester (4). One drop of a 3 M HCl was added to a stirred solution of 7 (11 mg, 0.02 mmol) in methanol (2 mL), and the solution was stirred at 45 °C for 4 h. After the mixture was cooled to room temperature, a half-saturated solution of $NaHCO_3$ (2 mL) was added and the aqueous layer was extracted with DCM (3 × 5 mL). The combined organic layers were dried ($MgSO_4$), and the solvent was removed under reduced pressure. To a stirred solution of crude triol (10 mg) in dry DCM (1 mL) at room temperature were added butyric anhydride (9.5 mg, 0.06 mmol) and 4-(dimethylamino)pyridine (DMAP) (catalytic amount). After being stirred at this temperature for 30 min, the reaction was quenched 3 M HCl (0.5 mL) and stirred for additional 20 min at the same temperature. The mixture was extracted with DCM (3 × 2 mL), and the combined organic layers were dried ($MgSO_4$), followed by evaporation the solvent under reduced pressure. The crude product was purified by flash chromatography (petrol/EtOAc, 2:1), which provided compound **4** (82% over two steps) as a clear transparent oil. HRMS (FAB+) *m/z* 519.2560 $[M + Na]^+$, $C_{26}H_{40}O_9Na$ requires 519.2570. $[\alpha]^{25}_D$ −20.9 (*c* 0.04, $CHCl_3$). ^{1}H NMR (500 MHz, $CDCl_3$) δ 6.08 (1H, qq, J = 1.5, 7.2 Hz, angeloyl, H-3), 5.40 (1H, dd, J = 8.5, 5.8 Hz, H-8), 5.05 (1H, d, J = 11.5 Hz, H-6), 4.85−4.79 (1H, m, H-3), 3.64−3.55 (2H, m, ethyl ether, H-1), 2.66−2.62 (1H, m, H-4), 2.54−2.48 (1H, m, H-1), 2.45−2.39 (1H, m, H-9), 2.28 (1H, t, J = 7.4 Hz, butanoyl, H-2), 2.09−2.05 (1H, m, H-5), 1.98 (3H, dq, J = 1.5, 7.2 Hz, angeloyl, H-4), 1.87 (3H, p, J = 1.5, angeloyl, C-2 CH_3), 1.79 (1H, dd, J = 8.8, 15.4 Hz, H-9′), 1.69−1.61 (3H, m, H-2, butanoyl H-3), 1.42 (3H, s, H-13), 1.29−1.25 (7H, m, H-2′, H-14, ethyl ether H-2), 1.17 (3H, d, J = 7.4 Hz, H-15), 0.87 (3H, t, J = 6.9 Hz, butanoyl H-4). ^{13}C NMR (125 MHz, $CDCl_3$) δ 174.1 (C-12), 171.0 (butanoyl, C═O), 167.7 (angeloyl, C═O), 138.7 (angeloyl, C-3), 127,6 (angeloyl, C-2), 81.7* (C-10), 81.3* (C-6), 80.0* (C-3), 79.9*-(C-7), 78.3*(C-11), 73.1 (C-8), 57.9 (ethyl ether, C-1) 46.7 (C-1), 44.5 (C-5), 43.3 (C-4), 38.3 (C-9), 36.3 (butanoyl, C-2), 31.9 (C-2), 26.8 (ethyl ether, C-2), 26.7 (butanoyl, C-3), 20.6 (angeloyl, C-2 *C*H_3), 18.2 (C-14), 18.1 (C-13), 16.5 (C-15), 16.3 (angeloyl, C-4), 13.6 (butanoyl, C-2).

(Z)-2-Methyl-but-2-enoic Acid (3*S*,3a*R*,4*S*,6*S*,6a*S*,8*R*,9*R*,-9a*R*,9b*S*)-6-Acetoxy-4-butyryloxy-3,3a-dihydroxy-3,6,9-trimethyl-2-oxo-dodecahydro-azuleno[4,5-b]furan-8-yl Ester (5). One drop of a 3 M HCl was added to a stirred solution of **9**[20] (14 mg, 0.03 mmol) in methanol, and the solution was stirred at 45 °C for 4 h. A half-saturated solution of $NaHCO_3$ (2 mL) was added to the solution after cooling to room temperature. The aqueous layer was extracted with DCM (3 × 5 mL). The combined organic layers were dried ($MgSO_4$), and the solvent was removed under reduced pressure. Butyric anhydride (9.5 mg, 0.06 mmol) was added to the crude product (11 mg) and DMAP (catalytic amount) dissolved in dry DCM (1 mL) at room temperature. After being stirred for 30 min, the reaction was quenched 3 M HCl (0.5 mL) and stirring continued for additional 20 min at the same temperature. The mixture was extracted with DCM (3 × 2 mL), and the combined organic layers were dried ($MgSO_4$), followed by evaporation the solvent under reduced pressure. The crude product was purified by flash chromatography (petrol/EtOAc, 2:1) providing compound 5 (9.7 mg, 63% over two steps) as a

colorless oil. HRMS (FAB+) *m/z* 533.2360 $[M + Na]^+$; $C_{26}H_{38}O_{10}$-Na requires 533.2363. $[\alpha]^{25}_D$ −57.7 (*c* 0.21, $CHCl_3$). ^1H NMR (300 MHz, $CDCl_3$) δ 6.03 (1H, qq, J = 1.5, 7.5 Hz, angeloyl H-3), 4.96 (1H, dd, J = 4.2, 6.6 Hz, H-8), 4.99 (1H, d, J = 10.5 Hz, H-6), 4.69 (1H, q, J = 7.2 Hz, H-3), 3.22 (1H, q, J = 9.0 Hz, H-1), 2.74 (1H, dd, J = 4.2, 15.0 Hz, H-9), 2.48−2.38 (1H, m, H-2), 2.37−2.29 (1H, m, H-4), 2.23 (2H, t, J = 6.9 Hz, butanoyl H-2), 2.10−2.02 (2H, m, H-5, H-9′), 1.96−1.92 (6H, m, acetyl H-2, angeloyl H-4), 1.83 (3H, p, J = 1.5 Hz, angeloyl C-2 CH_3), 1.63−1.54 (3H, m, H-2′, butanoyl H-3), 1.48 (3H, s, H-13), 1.37 (3H, s, H-14), 1.11 (3H, d, J = 7.2 Hz, H-15), 0.89 (3H, t, J = 7.2 Hz, butanoyl H-4). ^{13}C NMR (75 MHz, $CDCl_3$) δ 174.8 (C-12), 172.0 (butanoyl, C═O), 170.0 (acetyl, C═O), 168.0 (angeloyl, C═O), 138.7 (angeloyl, C-3), 127,9 (angeloyl, C-2), 86.3 (C-10), 81.9 (C-6), 79.7 (C-3), 79.6*(C-7), 79.0*(C-11), 70.1 (C-8), 45.0 (C-1), 44.4 (C-5), 44.2 (C-4), 39.4 (C-9), 36.7 (butanoyl, C-2), 33.7 (C-2), 25.8 (butanoyl, C-3), 22.9 (acetyl, C-2), 21.1 (angeloyl, C-2 CH_3), 18.4 (C-14), 18.2 (C-13), 17.1 (C-15), 16.3 (angeloyl, C-4), 14.1 (butanoyl, C-4).

Isolation of Sarcoplasmic Reticulum (SR). Preparation of SR vesicles containing Ca^{2+}-ATPases from rabbit muscle was done as previously described.[25] The SR vesicles were stored at −80 °C prior to use.

Measurement of SERCA Inhibitory Activity. All chemicals used in the assay were supplied by Sigma. UV absorbance was measure with a Multiskan EX microplate spectrophotometer from Labsystems, Finland. Buffer solution A: 0.1 M KCl, 20 mM Trizma-HCl, pH 7.5, 5 mM $MgCl_2$, 0.5 mM EGTA, 0.7 mM $MgCl_2$. The buffer A was used in the following three solutions. Solution 1: 1.2 mM β-NADH, 1.5 mM phosphoenolpyruvate, 4.5 μM A23187, 22.5 U/mL phosphoenolpyruvate kinase, 54 U/mL lactate dehydrogenase, and 30 μg/mL SR protein in buffer A. Solution 2: Inhibitor and control solutions was typically made in a 3 mM DMSO solution, which was diluted 1:100 in buffer A. The presents of DMSO did not affect the biological response. Serial dilutions were made using buffer A. Solution 3: 0.73 mM ATP in buffer A. 100 μL of solution 1 and 2 was mixed and to start the reaction 100 μL of solution 3 was added. This mixture was allowed to incubate for 3 min. At room temperature the OD_{340} was measured kinetically over a time period of 10 min. The Tg was used as a positive control. All measurements were performed in triplicate. After plotting the ATPase activity as a function of inhibitor concentration the IC_{50} value was estimated by fitting using the program Origin version 5.0 from Microcal Origin, Microcal Software Inc.

Computational Methods. All the calculations were performed on a SGI Octane workstation. Insight II version 2000 (Accelrys, Inc.) was used for visualization of the ligand−protein complexes and the GRID energy contours. The X-ray structure of the SERCA−thapsigargin complex was retrieved from the RCSB Protein Data Bank[26] (pdb code 1IWO).

GRID Analysis. Molecular interactions fields of selected probes were calculated for the X-ray structure in the pdb file 1IWO. The protein structure was carefully checked for inconsistencies and missing side chains or amino acids. The interaction energies were calculated by using GRID, version 20,[15] with the graphical interface GREATER, version 1.0.1 set to use default values except for keyword ALDM which was set to 1. The spacing of the grid was 0.333 Å and the grid dimensions, in Å,: X_{min}/X_{max} , −23.8/26.9; Y_{min}/Y_{max} , −43.2/1.1; Z_{min}/Z_{max} , −10.6/34.8.

To explore the lipophilic and hydrophilic characteristics of the binding site, two different probes were used: the methyl probe (C3) and the water probe (OH2). The calculations for the water probe were performed with as well as without the ligand, whereas the calculations for the methyl probe were only performed without the presence of the ligand.

Conformational Search and Docking. All calculations were performed using MacroModel version 8.1.[27] Energy minimization and conformation analyses were performed using the force field MMFF94s[28] and the TNCG energy minimization algorithm. Aqueous solvation was included through the generalized Born/solvent accessible surface area (GB/SA) continuum dielectric solvation model.[29] Low energy conformations were found using the Monte Carlo multiple minimum method (MCMM). The torsional angles in all three rings were varied during the conformational search by using the method of opening and reclosing of rings implemented in MacroModel. Default settings were used except for "maximum torsional rotation" which was set to 360°.[30] The search was continued until all low-energy conformations were found multiple times. Conformations with energies less than 25 kcal/mol above the calculated lowest energy minimum were saved. The Tg analogues were manually docked into the binding site using Insight II and employing Tg as a template.

Putative Active Sites Spheres (PASS) Analysis. The calculations of the volume and shape of the binding cavity was performed using the program PASS.[19]

Acknowledgment. This work was supported by the Danish Cancer Society, the Novartis Research Fellowship (to S.V.L.), the Royal Society (to M.D.S.), and the Wellcome Trust (to S.F.O.).

References

(1) Pinski, J.; Parikh, A.; Bova, G. S.; Isaacs, J. T. Therapeutic implications of enhanced G(0)/G(1) checkpoint control induced by coculture of prostate cancer cells with osteoblasts. *Cancer Res.* **2001**, *61*, 6372−6376.
(2) Berges, R. R.; Vukanovic, J.; Epstein, J. I.; CarMichel, M.; Cisek, L.; Johnson, D. E.; Veltri, R. W.; Walsh, P. C.; Isaacs, J. T. Implication of cell kinetic changes during the progression of human prostatic cancer. *Clin. Cancer Res.* **1995**, *1*, 473−480.
(3) Rasmussen, U.; Christensen, S. B.; Sandberg, F. Thapsigargin and Thapsigargicin, Two New Histamine Liberators from *Thapsia garganica* L. *Acta Pharm. Suec.* **1978**, *15*, 133−140.
(4) Lin, X. S.; Denmeade, S. R.; Cisek, L.; Isaacs, J. T. Mechanism and role of growth arrest in programmed (apoptotic) death of prostatic cancer cells induced by thapsigargin. *Prostate* **1997**, *33*, 201−207.
(5) Denmeade, S. R.; Jakobsen, C. M.; Janssen, S.; Khan, S. R.; Garrett, E. S.; Lilja, H.; Christensen, S. B.; Isaacs, J. T. Prostate-specific antigen-activated thapsigargin prodrug as targeted therapy for prostate cancer. *J. Natl. Cancer Inst.* **2003**, *95*, 990−1000.
(6) Tombal, B.; Weeraratna, A. T.; Denmeade, S. R.; Isaacs, J. T. Thapsigargin induces a calmodulin/calcineurin-dependent apoptotic cascade responsible for the death of prostatic cancer cells. *Prostate* **2000**, *43*, 303−317.
(7) Toyoshima, C.; Nakasako, M.; Nomura, H.; Ogawa, H. Crystal Structure of the Calcium Pump of the of Sarcoplasmic Reticulum at 2.6 Å Resolution. *Nature* **2000**, *405*, 647−655.
(8) Toyoshima, C.; Nomura, H. Structural changes in the calcium pump accompanying the dissociation of calcium. *Nature* **2002**, *418*, 605−611.
(9) Toyoshima, C.; Mizutani, T. Crystal structure of the calcium pump with a bound ATP analogue. *Nature* **2004**, *430*, 529−535.
(10) Sorensen, T. L.; Moller, J. V.; Nissen, P. Phosphoryl transfer and calcium ion occlusion in the calcium pump. *Science* **2004**, *304*, 1672−1675.
(11) Ma, H.; Lewis, D.; Xu, C.; Inesi, G.; Toyoshima, C. Functional and Structural Roles of Critical Amino Acids within the"N", "P", and "A" Domains of the Ca(2+) ATPase (SERCA) Headpiece. *Biochemistry* **2005**, *44*, 8090−8100.
(12) Davidson, G. A.; Varhol, R. J. Kinetics of thapsigargin-Ca(2+)-ATPase (sarcoplasmic reticulum) interaction reveals a two-step binding mechanism and picomolar inhibition. *J. Biol. Chem.* **1995**, *270*, 11731−11734.
(13) Thastrup, O.; Cullen, P. J.; Drøbak, B. K.; Hanley, M. R.; Dawson, A. P. Thapsigargin, a Tumor Promoter, Discharges Intracellular Ca^{2+} Stores by Specific Inhibition of the Endoplasmic Reticulum Ca^{2+}-ATPase. *Proc. Natl. Acad. Sci. U.S.A.* **1990**, *87*, 2466−2470.
(14) Christensen, S. B.; Andersen, A.; Smitt, U. W. Sesquiterpenoids from Thapsia Species and Medicinal Chemistry of the Thapsigargins. *Prog. Chem. Natl. Prod.* **1997**, *71*, 131−167.
(15) Goodford, P. J. A Computational Procedure for Determining Energetically Favorable Binding Sites on Biological Important Macromolecules. *J. Med. Chem.* **1985**, *28*, 849−857.
(16) Brady, S. F.; Pawluczyk, J. M.; Lumma, P. K.; Feng, D.-M.; Wai, J. M.; Jones, R.; DeFeo-Jones, D.; Wong, B. K.; Miller-Stein, C.; Lin, J. H.; Oliff, A.; Freidinger, R. M.; Garsky, V. M. Design and Synthesis of a Pro-Drug ov Vinbalstine Targeted at Treatment of Prostate CAncer with Enhanced Efficacy and Reduced Systemic Toxicity. *J. Med. Chem.* **2002**, *45*, 4706−4715.

(17) Singh, P.; Mhaka, A. M.; Christensen, S. B.; Gray, J. J.; Denmeade, S. R.; Isaacs, J. T. Applying Linear Interaction Energy Method for Rational Design of Noncompetitive Allosteric Inhibitors of the Sarco- and Endoplasmic Reticulum Calcium-ATPase. *J. Med Chem.* **2005**, *48*, 3005−3014.
(18) Paula, S.; Ball, W. J. Molecular determinants of thapsigargin binding by SERCA Ca^{2+}-ATPase: A computational docking study. *Proteins* **2004**, *56*, 595−604.
(19) Brady, G. P.; Stouten, P. F. W. Fast prediction and visualization of protein binding pockets with PASS. *Journal Comput.-Aided Mol. Des.* **2000**, *14*, 383−401.
(20) Ley, S. V.; Antonello, A.; Balskus, E. P.; Booth, D. T.; Christensen, S. B.; Cleator, E.; Gold, H.; Hogenauer, K.; Hunger, U.; Myers, R. M.; Oliver, S. F.; Simic, O.; Smith, M. D.; Sohoel, H.; Woolford, A. J. A. Synthesis of the thapsigargins. *Proc. Natl. Acad. Sci. U.S.A.* **2004**, *101*, 12073−12078.
(21) Oliver, S. F.; Högernauer, K.; Simic, O.; Antonello, A.; Smith, M. D.; Ley, S. V. A route to the thapsigargins from (*S*)-carvone providing a substrate-controlled total synthesis of trilobolide, nortrilobolide, and thapsiviollosin F. *Angew. Chem., Int. Ed.* **2003**, *42*, 5996−6000.
(22) Berger, M.; Mulzer, J. Total synthesis of tartrolon B. *J. Am. Chem. Soc.* **1999**, *121*, 8393−8394.
(23) Varga, S.; Mullner, N.; Pikula, S.; Papp, S.; Varga, K.; Martonosi, A. Pressure Effects on Sarcoplasmic-Reticulum. *J. Biol. Chem.* **1986**, *261*, 3943−3956.
(24) Seidler, N. W.; Jona, I.; Vegh, M.; Martonosi, A. Cyclopiazonic Acid Is A Specific Inhibitor of the Ca-2+-Atpase of Sarcoplasmic-Reticulum. *J. Biol. Chem.* **1989**, *264*, 17816−17823.
(25) Kosk-Kosicka, D. Measurement of Ca^{2+}-ATPase activity in PMCA and SERCA1. *Methods Mol. Biol.* **1999**, *114*, 343−354.
(26) Berman, H. M.; Westbrook, J.; Feng, Z.; Gilliland, G.; Bhat, T. N.; Weissig, H.; Shindyalov, I. N.; Bourne, P. E. The protein data bank. *Nucleic Acids Res.* **2000**, 235−242.
(27) Mohamadi, F.; Richards, N. G. J.; Guida, W. C.; Liskamp, R.; Lipton, M.; Caufield, C.; Chang, G.; Hendrickson, T.; Still, W. C. Macromodel − An Integrated Software System for Modeling Organic and Bioorganic Molecules Using Molecular Mechanics. *J. Comput. Chem.* **1990**, *11*, 440−467.
(28) Halgren, T. A. MMFF VI. MMFF94s option for energy minimization studies. *J. Comput. Chem.* **1999**, *20*, 720−729.
(29) Still, W. C.; Tempczyk, A.; Hawley, R. C.; Hendrickson, T. Semianalytical treatment of solvation for molecular mechanics and dynamics. *J. Am. Chem. Soc.* **1990**, *112*, 6127−6129.
(30) Chang, G.; Guida, W. C.; Still, W. C. An internal coordinate Monte Carlo method for searching conformational space. *J. Am. Chem. Soc.* **1989**, *111*, 4379−4386.

JM058036V